

PERSPECTIVE

CVD graphene with high electrical conductivity: empowering applications

To cite this article: Shuliang Lv et al 2025 2D Mater. 12 013003

View the article online for updates and enhancements.

You may also like

- Universal production of anisotropic bilayer WSe₂ nanoscrolls for high-performance photodetector Xiang Lan, Fen Zhang, Ziwei Huang et al.

- Towards invertible 2D crystal structure representation for efficient downstream

Egor Shibaev and Andrey Ustyuzhanin

Giant piezoelectricity in antiferromagnetic CrS₂ and CrSe₂ monolayers Yang Liu, Wei Wang, Zexuan Liu et al.

2D Materials



RECEIVED 4 June 2024

4 June 202

REVISED 9 August 2024

ACCEPTED FOR PUBLICATION 16 October 2024

PUBLISHED
29 October 2024

PERSPECTIVE

CVD graphene with high electrical conductivity: empowering applications

Shuliang Lv^{1,2,5}, Haihui Liu^{2,5,*}, Fuchao Yan¹, Wenhao Lu¹, Boyang Mao^{3,*} and Jincan Zhang^{1,2,3,4,*}

- College of Energy, Soochow Institute for Energy and Materials Innovations, SUDA-BGI Collaborative Innovation Centre, Key Laboratory of Advanced Carbon Materials and Wearable Energy Technologies of Jiangsu Province, Soochow University, Suzhou 215006, People's Republic of China
- ² School of Material Science and Engineering, Tianjin Key Laboratory of Advanced Fibers and Energy Storage, State Key Laboratory of Separation Membranes and Membrane Processes, Tiangong University, 300387 Tianjin, People's Republic of China
- ³ Department of Engineering, University of Cambridge, Cambridge CB3 0FA, United Kingdom
- ⁴ Beijing Graphene Institute, 100095 Beijing, People's Republic of China
- ⁵ Authors contributed equally to this work and should be considered co-first authors.
- * Authors to whom any correspondence should be addressed.

E-mail: liuhaihui@tiangong.edu.cn, bm573@eng.cam.ac.uk and jczhang2024@suda.edu.cn

Keywords: graphene, chemical vapor deposition, high electrical conductivity

Abstract

Graphene is an extraordinary material boasting a unique structure, enthralling properties, and promising application vistas. Particularly, the remarkable electrical conductivity of graphene confers it with an inimitable superiority in multiple fields. Endeavors have been continuously made to progressively elevate the conductivity of graphene materials that are synthesized using chemical vapor deposition (CVD), the primary means to prepare high-quality graphene in batches. From this perspective, we offer a comprehensive analysis and discussions on the growth, transfer, and post-treatment strategies evolved towards highly conductive graphene over the past five years. Large-area graphene films, ranging from monolayer to multilayer ones, are initially addressed, succeeded by graphene-based composites which enable traditional metals and non-metal materials to showcase novel or enhanced electrical performances. Eventually, an outlook for future directions to achieve higher electrical conductivity and to develop novel applications for CVD graphene materials is provided.

1. Introduction

Graphene, a remarkable two-dimensional material with a distinctive structure and captivating properties [1] has attracted extensive attention from both academia and industry, due to its auspicious application prospects in versatile fields, including electronics [2], photonics [3], optoelectronics [4], biomedicine [5], and environment energy [6]. Among various graphene preparation methods [7], chemical vapor deposition (CVD) is advantageous in mass production of high-quality graphene with fine controllability and large-area uniformity, as evidenced by the significant progress in both fundamental research and industrial production [8].

Electrical conductivity (σ) pertains to the capacity of an electric conductor to facilitate the internal current flow [9], which can be articulated as the product of carrier concentration (n) and carrier

mobility (μ), or the reciprocal of resistivity (ρ) [10]. In the case of graphene, the high σ , along with its tunability, holds great significance for its applications in electromagnetic interference shielding [11], energy storage [12], electrical-thermal conversion [13], field-effect transistors [14, 15] and electronic-photonic integrations [4]. The combination of high transparency and high σ in graphene endows it with enhanced competitiveness as a transparent conductor, for instance, as the flexible touch screen for mobile phones [6], the transparent electrodes for solar cells [16], or the smart windows for defogging and unfreezing using electrical heating [17].

Here, this perspective intends to furnish an indepth understanding of the preparation and application of highly conductive CVD graphene-based materials (figure 1). We first commence from the synthesis, transfer, and post-treatment of graphene film materials, and then shift to CVD graphene-based

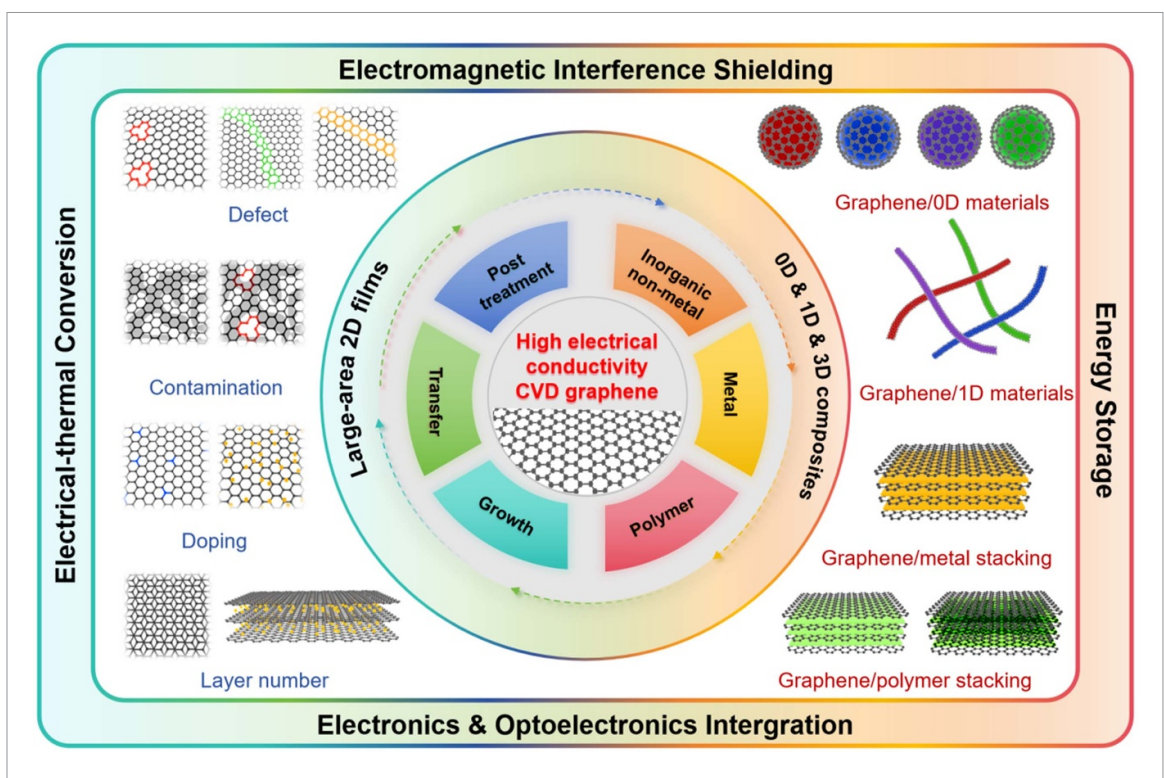


Figure 1. Controlled preparation and application prospects of highly conductive CVD graphene and its composites.

composites, for which the combination of graphene with metals, and non-metals is examined, by summarizing the most recent progress and novel tactics in enhancing the electrical conductivity of CVD graphene and its composites in the past five years. The application-oriented future research targets and development directions are finally provided.

2. Single-layer and multilayer CVD graphene films

For CVD graphene films, sheet resistance (R_s) is prevalently employed to depict its electrical conductivity. It is usually experimentally measured using a four-probe method [18] and calculated as

$$R_s = \frac{(V_{X_2} - V_{X_1})w}{Id}$$

where V_{X1} and V_{X2} are the voltage measured at voltage leads X_2 and X_1 , w is the channel width, d is the distance between the voltage leads X_2 and X_1 , and I is the current flowing between leads X_1 and X_2 [19, 20]. High σ , namely, low R_s , has been one of primary pursuits over the past decade, which can be attained by augmenting μ and n within graphene.

2.1. Synthesis

Through the control of the fundamental steps in the high-temperature CVD growth process, the conductivity of graphene films has been effectively enhanced by means of improving structural perfection, surface cleanness, or through controlling the layer number and stacking configuration, doping type and doping concentration (table 1). It is notable that Prof. Zhongfan Liu's group from Peking University and the Beijing Graphene Institute has conducted a succession of exemplary undertakings in this realm.

Defect, or structural imperfection within graphene lattice, such as point defects, wrinkles, and grain boundaries, has been extensively reported to result in low μ and consequently higher R_s [37]. Graphene films grown on metal substrates typically possess negligible defect density and low R_s (<500 Ω sq⁻¹), while graphene films directly grown on insulating substrates have numerous defects, bringing about $R_s > 1000 \Omega \text{sq}^{-1}$, even $>10\,000~\Omega \text{sq}^{-1}$ [6]. To minimize this disparity, several tactics have been devised to grow high-quality graphene films on non-metal substrates. For instance, Chen et al designed an electromagnetic induction heating CVD operating at an ultrahigh temperature (>1300 °C), and obtained a highly oriented singlelayer graphene (SLG) film with significantly reduced R_s of $\sim 587 \Omega \text{sq}^{-1}$ on a sapphire wafer, a recordbreaking outcome for SLG directly grown on nonmetal substrates. To actualize transfer-free growth of wafer-scale graphene, Shan et al used copper acetate as precursor to continuously supply gaseous Cu catalysts for graphene growth on sapphire wafers [31], and Jiang et al grew ultra-flat graphene films at 1230 °C on quartz glass wafers [32]. For large-area growth of graphene on quartz plates, a CO2-assisted

 $\textbf{Table 1.} \ \textbf{CVD} \ \textbf{synthesis} \ \textbf{of} \ \textbf{graphene} \ \textbf{films} \ \textbf{with} \ \textbf{improved} \ \textbf{electrical} \ \textbf{conductivity}.$

Year	Layer number	$R_s/\Omega \mathrm{sq}^{-1}$	Strategies	Growth substrates	Measurement substrates	t Journals	References
2019	1	1,000-3,000	Cu-foam assisted plasma-enhanced CVD to decrease defect density	Glass		J. Mater. Chem. A	[21]
2019	1	269 ± 70	Continuous supply of Cu vapor to inhibit the formation of surface contamination	Cu foil	SiO ₂ /Si	Nat. Commun.	[22]
2019	1	270 ± 30	Improve graphene cleanness via using Cu(OAc) ₂ as precursor	Cu foil	SiO ₂ /Si	J. Am. Chem. Soc.	[23]
2019	1	390 ± 110	Selectively etch surface contamination using CO ₂	Cu foil		Angew. Chem. Int. Ed.	[24]
2019	1	130 ± 20	Introduce nitrogen cluster doping	Cu foil	SiO ₂ /Si	Sci. Adv.	[25]
2020	1	450 ± 60	Improve graphene cleanness by using cold-wall CVD to inhibit gas-phase by-reactions	Cu foil		Angew. Chem. Int. Ed.	[26]
2020	1	2,000 ± 200	Optimize comprehensive growth parameters and wafer spacing in periodic alignment to decrease defect density	Quartz wafers		Nano Res.	[27]
2021	1	900	Oxygen-assisted direct growth to decrease defect density	Quartz glass		Nano Res.	[28]
2021	1	587 ± 40	Electromagnetic inductive heating to minimize its configuration energy to decrease defect density	Sapphire wafers		Sci. Adv.	[29]
2022	1	1,409 ± 117	Using an interface-decoupling CVD strategy	Si wafer		Adv. Mater.	[30]
2022	1	1,240 ± 70	Cu(OAc) ₂ -promoted transfer-free growth of high-quality graphene with decreased defect density	Sapphire or quartz		Natl. Sci. Rev.	[31]
2022	1	750 ± 210	Control flatness of the substrate to avoid forming multilayer structures	Quartz glass		Adv. Funct. Mater.	[32]
2023	1	1,220 ± 80	Construct stacked substrate configurations to decrease defect density	Quartz		Adv. Funct. Mater.	[33]
2023	1	$1,260 \pm 350$	CO ₂ promotes the transfer-free direct growth of graphene with decreased defect density	Quartz		Nano Res.	[34]
2023	1 2	339 ± 44 150 ± 21	Introduce trace amount of CO ₂ to grow BLG	Cu foils	SiO ₂ /Si	Nat. Commun	. [35]
2023	2	344 ± 49	Well-tune alloy thickness and strain to acquire wrinkle-free BLG	CuNi(111)/sapphire	SiO ₂ /Si	Nano Res.	[36]

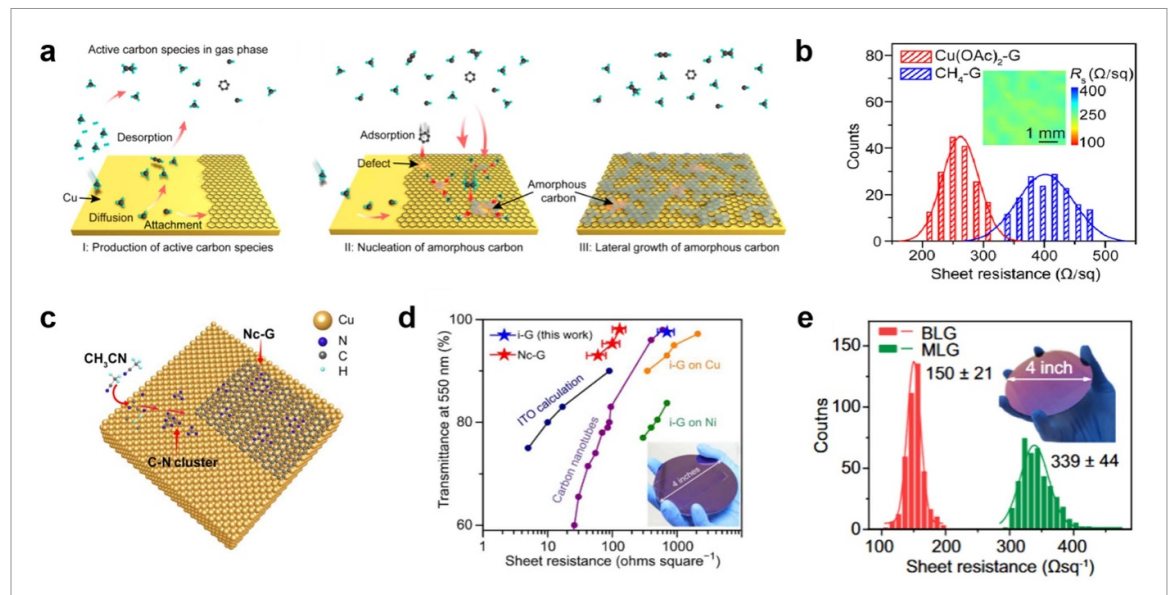


Figure 2. CVD synthesis of graphene film with high conductivity. (a) Schematics of the formation mechanism of amorphous carbon on graphene surface during high-temperature growth. Reprinted with permission from [42]. Copyright (2020) American Chemical Society. (b) Statistical results of R_s of graphene grown using Cu(OAc)₂ (red) and CH₄ (blue). Reprinted with permission from [23]. Copyright (2019) American Chemical Society. (c) Illustration of the Nc-G film formation. (d) R_s versus optical transmission (at 550 nm) for the Nc-G films and a pristine graphene film (i-G) with \sim 1 mm domain size for contrast. From [25]. Reprinted with permission from AAAS. (e) Statistical histograms of the R_s of the SLG (green) and BLG (red) transferred onto SiO₂/Si substrates. Reproduced from [35]. CC BY 4.0.

strategy has been put forwards reduce the energy barrier of CH₄ decomposition and carbon adsorption to the growth frontier [34], which can also be achieved with the aid of hydroxyl groups released from quartz surface at high temperature, producing graphene films with good batch uniformity on 12 inch sized fused silica [33].

For graphene on metal substrates, the elimination of graphene boundaries and wrinkles, that is, the synthesis of wrinkle-free single-crystalline graphene, is more efficacious in reducing the R_s of graphene, which also enhances the large-area uniformity of its electrical properties [38]. Deng *et al* firstly reported wrinkle-free single-crystal graphene growth on Cu(111)/sapphire through strain engineering in 2017 and reported R_s to 275 Ω sq⁻¹ [39]. Recently, Zhu *et al* accomplished the controllable synthesis of high-quality single crystal graphene wafers on single crystal Cu(111)/sapphire substrates, which have a uniform R_s with a deviation of \sim 5%, further indicating the significance in eradicating grain boundaries [40].

Surface contamination is intimately associated with lattice defects and exerts a detrimental influence on the intrinsic properties of graphene [41–43]. Moreover, In comparison with the unclean graphene, the surface polymer residues on superclean graphene are conspicuously reduced after transfer, further indicating the significance to grow superclean graphene [42]. The formation mechanism of graphene surface contamination is depicted in figure 2(a) [42]. Introducing gas-phase Cu catalyst during the high-temperature growth process is

the key to synthesize superclean graphene, which has been achieved via using Cu foam [6] or copper acetate to provide sufficient Cu vapors during growth [23]. The as-grown clean graphene exhibits a narrow R_s distribution with an average value of $270 \, \Omega \text{sq}^{-1}$ (figure 2(b)). Zhang *et al* further obtained large-area superclean graphene film via selective CO_2 etching at mild temperature, which has fine compatibility with mass production process [24]. In addition, cold-wall CVD has been verified to be more advantageous in synthesizing superclean graphene than hot-wall CVD, owing to the inhibited formation of large hydrocarbon clusters [26].

Compared with SLG, bilayer graphene (BLG) has enhanced electrical conductivity and mechanical strength [44]. Using Cu(111)/sapphire substrates, Wang *et al* synthesized a centimeter-sized BLG film via designing a confined space with tunable gap [45] and Tang *et al* achieved ultrafast growth of wafer-level wrinkle-free AB-stacking BLG wafers with $R_s \sim 344 \pm 49~\Omega \text{sq}^{-1}$ [36]. Zhang *et al* introduced a trace amount of CO₂ during the high-temperature growth process and achieved fast preparation of meter-sized BLG films on commercial polycrystalline Cu foils. The R_s of BLG (\sim 150 Ωsq^{-1}) is significantly lower than that of SLG (\sim 339 Ωsq^{-1}) (figure 2(e))

Doping changed the Fermi level of graphene and thus increased its n, which thereby contributes to low R_s . Bianco $et\ al$ used layer-by-layer CVD method to grow n-doped graphene on copper foil. The results show that the R_s of light-irradiated nitrogen-doped

graphene is significantly reduced, and the trilayer graphene (TLG) has a lowest R_s of $\sim 100~\Omega \text{sq}^{-1}$ [46]. To obtained doped graphene with both high μ and high n, Lin et~al synthesized in-plane graphite nitrogen cluster doped graphene (Nc-G) with millimetersized single crystal domains (figure 2(c)). The clustering of dopants in graphene significantly reduces the scattering of carriers by dopants and thus increases the conductivity [47]. The film showed an average R_s value of 130 Ωsq^{-1} and a minimum $< 100~\Omega \text{sq}^{-1}$ (figure 2(d)) [25], the best value for CVD-grown SLG without post-doping treatment.

2.2. Transfer and post-treatment

CVD graphene films usually grow on metal substrates, like Cu foils, and thus needs to be transferred onto functional substrates for practical utilization. Hence, the transfer technology remains a crucial means for integrating two-dimensional materials into the existing device architectures [48]. Hereinafter, the focus is placed on the recent research progress in accordance with the characteristics of the target functional substrates, auxiliary support media, and doping control during the transfer process (table 2) [16, 49].

The Polymethyl methacrylate (PMMA)-assisted wet transfer method has been developed and prevalently employed in the past decade; nevertheless, it possesses distinct drawbacks, such as inferior controllability in doping and strain. To address this, Gao et al devised a multifunctional three-layer transfer medium with a gradient surface energy distribution to incorporate 4-inch single crystal ultra-flat graphene onto silicon wafers. The transferred graphene sheets preserve their planarity, presenting a complete and clean surface, along with an extremely uniform R_s of $\sim 655 \pm 39 \ \Omega \text{sg}^{-1}$ (standard deviation of only 6%) and an average μ exceeding 100 000 cm² V⁻¹ s⁻¹ on a 4 inchsized wafer [59]. Zhao et al achieved conformal contact between graphene and the target substrate by adding hydroxyl-containing volatile molecules or low glass transition temperature polymers to PMMA, and realized the transfer of 4-inch-sized graphene single crystal wafers on rigid SiO2/Si and flexible plastic substrates (figures 3(a) and (b)). The large-area crack-free, pollution-free, and wrinklefree transfer, followed by the blade coating of poly (3,4-ethylenedioxythiophene): polystyrene sulfonate (PEDOT:PSS) reduces the R_s to 87 \pm 13 Ω sq⁻¹ (figure 3(c)), with an optical transmittance of 92.3% [59].

The purposeful introduction of dopants during transfer process is facile and efficacious in enhancing the electrical conductivity of graphene. For example, Seo *et al* employed a soft amine-rich thin gel buffer as a shock-absorbing binder and an *n*-type doping layer to mechanically exfoliating graphene directly

from a metal substrate without damage. After coupling the amine-rich polyethylenimine-glutaraldehyde (PEI-GA) layer to graphene surface, electrons are injected into the graphene from PEI molecule with electron lone pair electrons in the amine group (figure 3(d)). Amine-rich gel with high optical transparency significantly reduces the R_s of graphene without compromising its optical transmittance. The average R_s of transferred graphene is $257 \pm 16 \, \Omega \text{sq}^{-1}$ on SiO_2/Si substrates [56].

Common dopants encompass metals, metal oxides and conductive polymers, functioning in the guises of clusters, nanowires, nanoplates or thin films [64, 65]. Vaziri *et al* achieved ultra-high and stable *p*-doping on graphene by growing a stoichiometric crystalline MoO₃ film on a CVD

SLG via vapor deposition (figure 3(e)) [53]. Choi et al realized high-density p-doping of graphene by using the work function-mediated charge transfer of single-layer tungsten oxyselenide and thus obtained R_s is <50 Ω sq⁻¹ for four-layer graphene [54]. Ma *et al* demonstrated a UV-epoxy adhesive to in-situ introduce strong p-doping using $HSbF_6$ (figure 3(f)) which reduces R_s by $\sim 60\%$ and to a value of $146 \pm 7 \Omega \text{sq}^{-1}$ at high transparency of 96.7% and with high stability [66]. Xu et al doped SLG and MLG by chemical modification using HCl and AuCl₃, effectively decreases R_s of TLG to 150 Ωsq^{-1} while keeping the optical transmittance in the visible range >91% [68]. Grande et al used thionyl chloride (SOCl₂) as a dopant molecule to dop CVD graphene layer by layer and prepare doped multilayer (MLG). For 6-layer graphene, $R_s \sim 12 \ \Omega \text{sq}^{-1}$ was obtained at 85% transmittance, which is a new record of this type of structure [50]. After HNO₃ doping, the R_s of seven layer graphene (7LG) decreased sharply to 36.6 Ω sq⁻¹, but the transparency was sacrificed [69]. Deng et al demonstrated continuous roll-to-roll production of transparent conductive flexible plastic based on AgNW network fully encapsulated between SLG and plastic substrate, resulting in superior optoelectronic properties (R_s of $\sim 8~\Omega \text{sq}^{-1}$ at 94% transmittance) [70], comparable to the performance of commercial transparent conductor (indium tin oxide, ITO).

Araki *et al* studied the effect of stacking angle on the intercalation of metal chlorides by preparing artificially stacked BLG with controllable torsion angles. The mixture of AlCl₃-CuCl₂ was intercalated into BLG. Due to the increase of hole concentration, the insertion of metal chlorides leads to a significant increase in the conductivity of the host BLG. Especially, R_s exhibits strong dependence on the twist angle, with the lowest value of 48 Ω sq⁻¹ for BLG with 30° twist intercalation [62]. Hiroki Ago used molybdenum chloride (MoCl₅) continuous intercalation to study the effect of stacking sequence on the R_s of large-area BLG and found that the twist-rich BLG sheet (red) exhibits lower R_s than the BLG sheet

 Table 2. Recent progress in transfer of CVD graphene films to achieve high electrical conductivity.

	Layer number	$R_s/\Omega \mathrm{sq}^{-1}$	Strategy	Measurement substrate	Journal	Group	References
2019	6	12	Layer-by-layer doping	Glass	Graphene 2019	G Bruno	[50]
2019	1	618.0 ± 19.6	Selectively removing surface contamination	SiO ₂ /Si	Adv. Mater.	Z F Liu	[51]
2020	1/12	280/25	Adjust the number of layers and interlayer doping state	SiO ₂ /Si	ACS Appl. Mater. Interfaces	Ki-Bum Kim	[52]
2020	1	230	Direct growth of polycrystalline MoO ₃ on graphene using fast flame synthesis technique	SiO ₂ /Si	npg Asia Mater.	E Pop	[53]
2021	4	50	Tungsten oxyselenide doping	SiO ₂ /Si	Nat. Electron.	J T Teherani	[54]
2020	1	96 ± 4	Synergistic electrical/optical modulation strategy	SiO ₂ /Si	Proc. Natl. Acad. Sci.	W C Ren	[55]
2021	1	258.8 ± 12.5	Use soft amine-rich thin gel buffer as <i>n</i> -type doping layer	PEI-GA/SiO ₂ /Si	ACS Nano	D Whang	[56]
2021	1	453 ± 13	Introduce compressive strain accelerates graphene exfoliation and the structural integrity is well preserved	Epoxy/PET	Adv. Funct. Mater.	W C Ren	[57]
2021	1	80 ± 5	Direct and polymer-free transfer	PET	J. Mater. Chem. C	Z P Liu	[58]
2022	1	87 ± 13	Introduce volatile molecules containing hydroxyl groups	SiO ₂ /Si	Nat. Commun.	Z F Liu	[59]
2022	1	600 ± 132	Design multifunctional three-layer transfer medium with gradient surface energy distribution		Nat. Commun.	H L Peng	[60]
2022	1	139.91 ± 6.24	Dual side doping with Benzimidazole (bottom) and AuCl ₃ (top)	SiO ₂ /Si	Appl. Surf. Sci.	S K Bae	[61]
2022	2	48 ± 50	Artificially stacking BLG with a controllable twist angle	SiO ₂ /Si	ACS Nano	H Ago	[62]
2022	3	100	Effective <i>p</i> -doping by the selective photochemical activation of N-oxypyridine and pyridone by pyridine nitrogen	SiO ₂ /Si	Sci. Rep.	G V Bianco	[46]
2023	1	574 ± 28	Polymer-assisted wet transfer and eliminated in-plane twin boundaries	SiO ₂ /Si	Adv. Mater.	Z F Liu	[40]
2023	1	193 ± 13	Combine frustrated Lewis pair doping with nanostructure engineering	SiO ₂ /Si	Nano. Res	W C Ren	[63]

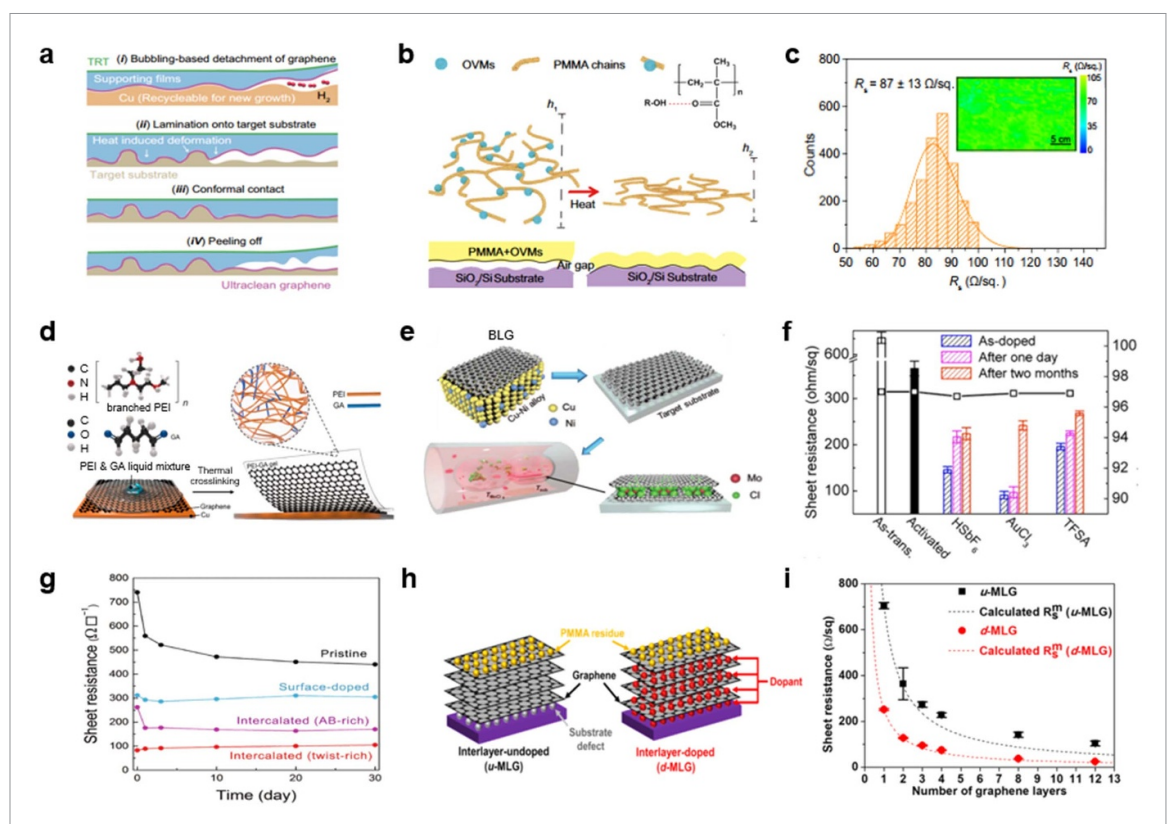


Figure 3. Improved electrical conductivity of graphene film via transfer and post-treatment. (a) Illustration of graphene transfer onto target substrates free of cracks and contamination. (b) Mechanism illustration of the heat-induced deformation and resulted conformal contact. (c) R_s statistics of graphene on PET substrates doped by PEDOT: PSS. Reproduced from [59]. CC BY 4.0. (d) Schematic illustration of the PEI-GA gel-assisted graphene transfer process. Reprinted with permission from [56]. Copyright (2021) American Chemical Society. (e) Schematic of the MoCl₅ intercalation in CVD-grown BLG. Reprinted with permission from [66]. Copyright (2018) American Chemical Society. (f) Comparison of the R_s and optical transmittance (R_s = 550 nm) of the UV-epoxy-transferred graphene films before and after surface doping with different dopants. Reprinted with permission from [67]. Copyright (2017) American Chemical Society. (g) Time dependence of R_s of BLG. Reprinted with permission from [66]. Copyright (2018) American Chemical Society. (h) Schematic diagram of u-MLG and u-MLG. There are interlayer surface residues for u-MLG, whereas for u-MLG, benzimidazole molecules are adsorbed between the graphene layers. (i) Dependence of R_s on layer numbers of u-MLG (black) and u-MLG (red). (Reprinted with permission from [52]. Copyright (2020) American Chemical Society.

(pink) containing AB (figure 3(g)). In specific, such twist-rich BLG film exhibits a very low R_s of 83 Ω sq⁻¹ while maintaining high optical transparency (\approx 95%) [67].

The electrical conductivity of graphene film increases with its layer number (N), following the rule that R_s of MLG is 1/N of that of SLG. Nevertheless, the reported R_s values of MLG are typically considerably larger than the predicted ones. For instance, Kim et al reported that the R_s of SLG to 7LG reduced from 512.5 Ω sq⁻¹ to 150.6 Ω sq⁻¹ [69]. To address this, the effect of inhomogeneity of each sublayer on the electrical properties of stacked graphene was also studied by adjusting the number of layers and the doping state between layers. In order to prepare MLG with diverse interfaces, two distinct layer stacking methods were employed. One is the layer-by-layer stacking transfer without residues at the interface to minimize unnecessary doping effects (u-MLG); the other is the interlayer doping using p-type dopant, benzimidazole during individual layer transfer (d-MLG) (figure 3(h)). As N increases from 1 to 12, the R_s

of *u*-MLG and *d*-MLG decreases from $705~\Omega \text{sq}^{-1}$ to $104~\Omega \text{sq}^{-1}$ and from $250~\Omega \text{sq}^{-1}$ to $25~\Omega \text{sq}^{-1}$, respectively (figure 3(i)), verifying that interlayer doping is more efficient [52].

3. CVD-graphene based composites

Graphene-based materials have been utilized in diverse forms ranging from zero-dimensional to three dimensional (3D), such as graphene quantum dots, nanobelts and foams [71, 72]. The unique atomic arrangement of carbon atoms in graphene makes it easy for electrons to travel at extremely high speeds without scattering, thereby saving valuable energy that is usually lost in other conductors. Therefore, graphene has excellent electrical properties, high electron mobility and variability of electrical properties. It thus has unique advantages to act as either substrate or filler when preparing composite materials with enhanced electrical conductivity. Through the incorporation of graphene reinforcements, traditional materials, such as metals, fibers, ceramics,

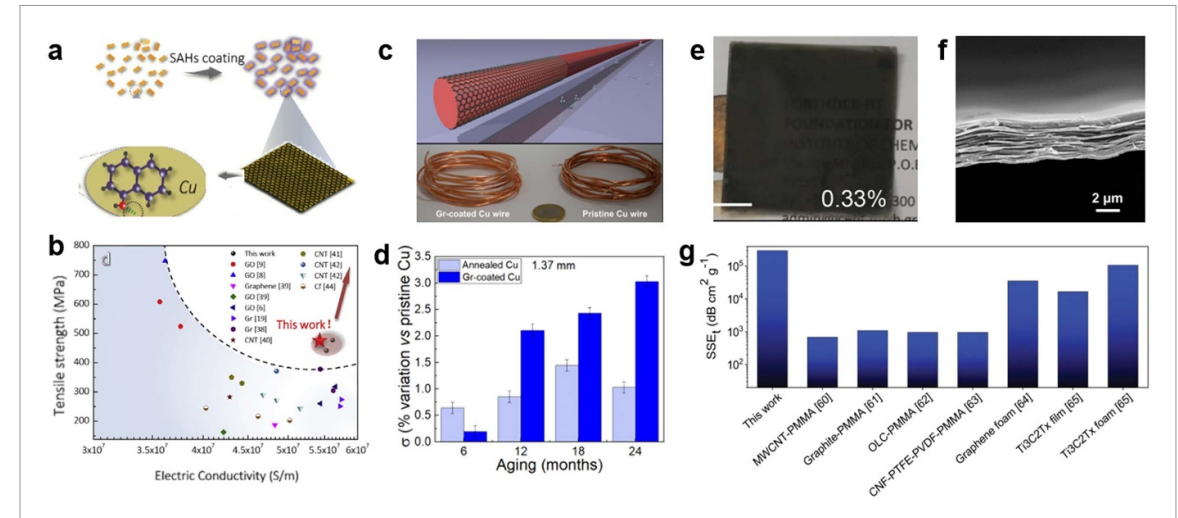


Figure 4. CVD-graphene based composites with high electrical conductivity. (a) Morphological properties of pristine and Gr-coated Cu cables. (b) Ultimate tensile strength versus electric conductivity of Cu matrix composites in comparison with other works. Reprinted from [75], Copyright (2019), with permission from Elsevier. (c) Schematic diagram of the preparation of graphene/Cu composite powders. (d) Electrical conductivity improvement of annealed and Gr-coated Cu with respect to pristine wires from 6 to 24 months of age. Reproduced from [76]. CC BY 4.0. (e) Representative images of cm-sized graphene/PMMA laminates. scalebar: 1 cm. (f) Cross-section SEM image of the laminates. (g) Comparison of SSE_t values between graphene/PMMA nanolaminates and state-of-the-art shielding materials in the THz range. (e)–(f) Reproduced from [11]. CC BY 4.0.

and polymers, have manifested enhanced or distinctive properties [73, 74]. This section will primarily focus on the augmented electrical properties of CVD graphene-based composites.

3.1. CVD graphene/metal composites

Except metal foils and films, direct CVD growth of graphene on metal nanoparticles and wires also attracts intense attentions, which has been reported to improve the overall performance of metal substrates. Wang et al synthesized graphene on Cu powders by adsorbing small molecule aromatic hydrocarbons, and the as-prepared graphene/Cu composite exhibits a high conductivity of $\sim 56.2 \times 10^6 \text{ Sm}^{-1}$ (figure 4(a)). Additionally, a good balance between strength and conductivity was achieved (figure 4(b)) [75]. Mishra *et al* demonstrated that Cu wires (CuWs) with diameters of 1.37 and 1.74 mm, which are frequently employed for low-voltage applications, can be effectively coated with graphene through scalable and industrially compatible CVD processes (figure 4(c)). It was found that the improvement of conductivity of thermal annealed Cu wires was poorer than that of graphene-coated Cu wires. Moreover, the graphenecoated copper wire showed good oxidation resistance, thereby increasing the conductivity (figure 4(d)) by up to 1% immediately after coating and up to 3% after 24 months, allowing the decrease of wire diameter to decrease, which would significantly lower the production cost [76]. Wang et al directly synthesized vertical graphene (VG) on CuWs by plasma enhanced CVD. Due to the high water contact angle of the hydrophobic VG coating, the corrosive liquid and water can

be effectively excluded from the CuWs surface to prevent further penetration [77].

Large-area graphene films can be embedded into metals (Cu, Al and Ag) foils to fabricate graphene/metal laminates. Cao *et al* deposited SLG on both sides of commercial Cu foils via CVD method, and then prepared graphene/Cu composites that exhibit ultra-high electrical conductivity of up to 58.1 × 10⁶ Sm⁻¹ by stacking and hot pressing the layers of SLG/Cu/SLG [78]. Zheng *et al* prepared Cu/graphene-Al-Cu/graphene (Cu/Gr-Al-Cu/Gr) laminated composites by ingenious hotpressing design. The increased number of graphene layers is beneficial for enhancing the electrical conductivity of the Cu/Gr-Al-Cu/Gr composite, and the conductivity up to 20.5% in comparison to that of raw Al [79].

3.2. CVD graphene/non-metal composite

The conjugation of graphene with fibers amalgamates the excellent electrical attributes of graphene and the pliability of fiber to enhance the overall performance of the composites. Cui *et al* contrived and mass-produced a hybrid configuration of graphene quartz fiber (GQF) via a forced-flow CVD method, which coalesces the excellent conductivity of graphene and the extraordinary properties of quartz fiber. The massively produced GQFs can be knitted into meter-scale fabrics with tunable conductivity (R_s ranging from 200 to 10 000 Ω sq⁻¹) and superior electrothermal conversion efficiency (reaching up to 980 °C within a few seconds at 24 V) [80]. Liu *et al* devised a complementary CVD

graphene growth strategy based on the synchronous introduction of mixed carbon precursors with high and low decomposition energy barrier. Through this approach, a large-area uniform graphene glass fiber fabric (GGFF) with a significantly reduced nonuniformity coefficient is fabricated [81]. The GGFFbased heater exhibits a widely adjustable temperature range (20 \sim 170 $^{\circ}$ C) at a low working voltage (<10 V) and uniform large-area heating temperature $(171.4 \pm 3.6 \,^{\circ}\text{C} \text{ in a 20 cm} \times 15 \,\text{cm area})$. The thickness of the as-grown graphene film increases with the prolonged growth time, resulting in the R_s decreasing to 49.33 \pm 0.64 Ω sq⁻¹ after 60 min growth. Xie et al prepared a 10 m \times 0.5 m flexible, highly conductive and ferromagnetic graphene quartz fabric with ultra-wideband strong EMI shielding effectiveness using CVD method. The highly conductive graphitic N-doped graphene layer (\sim 3,906 Scm⁻¹) shows the strong reflection ability of electromagnetic waves [82].

At the same time, CVD synthesis of graphene on 3D non-metal substrates was also accomplished to make the insulating substrates become conductive. For instance, Ramírez et al prepared honeycomb graphene/Al₂O₃ hybrid materials via catalystfree CVD graphene growth on highly porous 3D printed patterned alumina scaffolds. The composite structure has a high conductivity of $10^1 \sim 10^3 \text{ Sm}^{-1}$, thanks to the continuous graphene/graphite network on the alumina surface, thus broadening the application of intrinsic insulating materials [83]. Markedly, the nanostructures of 3D graphene are different from other kinds, due to the interconnected porous networks of two-dimensional graphene sheets. Zeng et al realized the growth of VG in a thermal CVD reactor and developed a new type of 3D graphene structure, namely 3D graphene fibers (3DGFs). The group found that the conductivity of the 3DGFs membrane was the highest after 35 h grown, reaching 1.2×10^5 Sm⁻¹, exceeding that of original carbon nanofibers (~184 Sm⁻¹) [84]. Wang et al prepared high-quality 3D graphene using bovine ash, a cheap and easily available biological waste, as template [71]. The as-obtained graphene skeleton is continuous, making it an excellent conductive skeleton for electrons and ions in electrochemical devices. Through uniformly compounding the S cathode on the 3D graphene, the performance of the Li-S battery was verified to be significantly superior to that of the Li-S battery using reduced graphene oxide as the conductive skeleton. Thanks to its high electrical conductivity, high specific surface area and good catalyst ability, 3D graphene has been widely utilized in energy storage fields, such as batteries and supercapacitors. It also shows great potential in hydrogen energy fields, including hydrogen generation, storage and utilization.

Another prospective application format of CVD graphene is incorporation into polymer. Graphene/polymer composites are competitive in electromagnetic shielding applications. This is because that graphene-based fillers can significantly improve the electrical, thermal and mechanical properties of polymer composites and thus improve the overall performances of polymers. For example, Pavlou et al prepared cm-sized CVD graphene/polymer laminates (figures 4(e) and (f)) with a very high shielding efficiency (SSE_t) value, reaching close to $3 \times 10^5 \text{ dB cm}^2 \text{ g}^{-1}$ (figure 4(g)), superior to the reported SSE, values measured using other nonmetallic shielding materials [11]. Recently, Kim et al proposed a more scalable manufacturing method, namely a floating stacking strategy, to prepare multifunctional graphene/PMMA laminates. As a result, highly crystalline semi-infinite graphene fillers are uniformly arranged in the polymer matrix, maximizing the reinforcing efficiency of the graphene filler [85].

4. Perspective

A comprehensive apprehension regarding the preparation and application of highly conductive CVD graphene-based materials is proffered, focusing on the latest advancements and novel strategies reported over the past five years. We initially commence from the synthesis, transfer, and post-treatment of graphene film materials, and subsequently segue to CVD graphene-based composites, for which the combination of graphene with metals and non-metals is deliberated. The application-oriented future research objectives and development directions are finally expounded.

In respect of material preparation, although structural imperfection matters have been addressed at the laboratory level, there remains a disparity towards the mass production and commercialization, particularly when contemplating the exigency to produce large-area graphene films with fine controllability, uniformity, and reproducibility (figure 5(a)). For instance, the existence of surface contaminants remains a significant factor influencing the inherent excellent performance of graphene, which requires to be resolved from both the growth and transfer stages. Multilayer graphene is advantageous in enhancing both the mechanical strength and electrical conductivity of graphene films while its large-area fast synthesis with controlled twist angles and negligible wrinkles densities still requires further efforts. We contrasted the three principal steps in the CVD graphene-related process for preparing highly conductive graphene films from five aspects, namely cost, quantity, stability, reproducibility, and environmental friendliness, all of which determine the

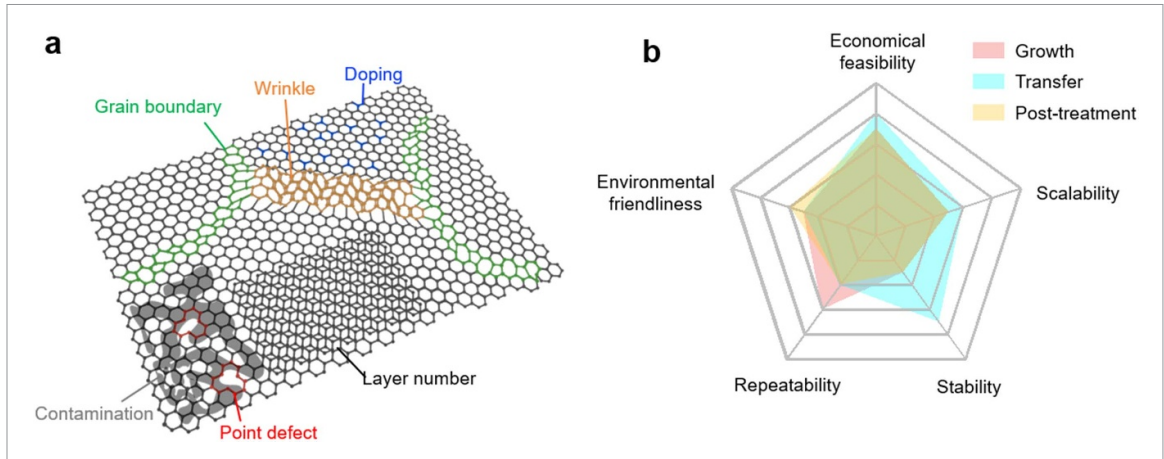


Figure 5. Approaches to prepare highly conductive CVD graphene films. (a) Structure control of CVD graphene films. (b) Comparison of three steps in tuning graphene's electrical conductivity.

potential of graphene to be incorporated into industrial utilization (figure 5(b)). It needs to be pointed out that future efforts to develop new material synthesis strategies should pay more attentions to improve scalability, stability, uniformity and repeatability, and to decrease the cost, rather than only focusing on improving hero electrical conductivity values. Such a tendency has been mirrored in the past years. Greater attention has been accorded to graphene-based composites, such as graphene/Cu wires, graphene glass, and graphene/PMMA laminates. Particularly, the concept of super graphene-skinned materials has unlocked more potentialities for making the optimal utilization of graphene [73, 74].

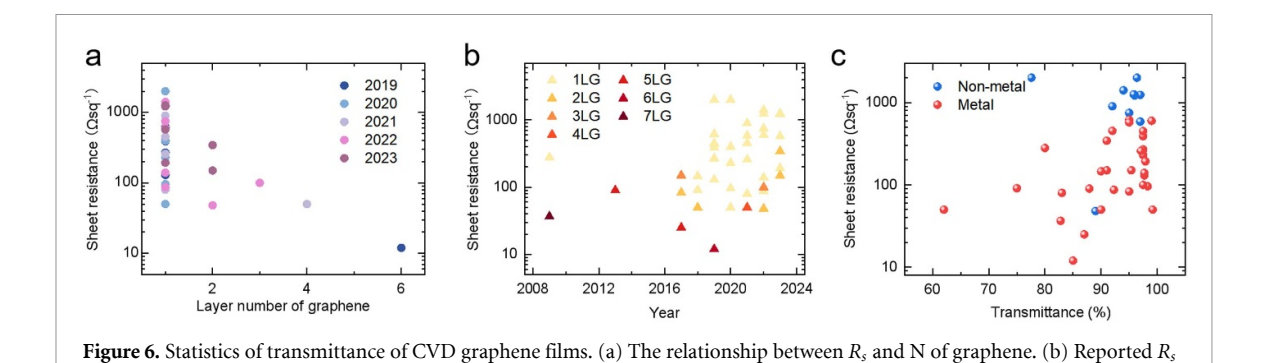
In the aspect of practical applications, the challenges regarding large-scale production and commercialization of CVD graphene remain to be addressed. Large-area high-quality graphene film possesses promising application vistas in the realm of integrated electronics and optoelectronics, such as transistors, displays, modulators, and sensors. Concurrently, graphene-based composites are more apt for flexible wearable apparatuses, highperformance fibers, sensors, etc. Different applications have disparate requirements and criteria for the quality and performance of graphene. For instance, the mobility of graphene is one of the prime considerations in electronics and optoelectronics applications, while for transparent conductors, optical transmittance and conductivity are the two main salient concerns. Products like high-frequency electronic devices, flexible displays, and sensors have entered the market and are anticipated to achieve mass production and utilization. In addition, application of CVD graphene and its composite in the energy fields is still in a relatively primary stage, mainly limited by the material preparation cost and process compatibility. Referring to Pt-C or Cu-C based

commercial catalysts, one-step low-temperature synthesis of graphene-metal catalyst composites by using graphene as the coating layer or support skeleton might provide more possibilities. However, the commercialization of CVD graphene films in these fields is still in its incipient stage and demands more input.

In all, the improvement of electrical conductivity in CVD graphene films is limited (figure 6(a)), with the majority of research concentrating on SLG (figure 6(b)). To make further breakthrough, novel strategies are highly required. For SLG, dual-side doping and control through three steps are more efficient while for MLG, the interlayer doping is vital to increase its electrical conductivity. From the perspective of growth substrates, the electrical conductivity of graphene films grown on metals, particularly Cu substrates, is significantly higher compared to that of graphene synthesized on non-metal insulating substrates (figure 6(c)). For the latter, growth at ultrahigh temperature is a tendency to improve SLG quality and introduction of post-treatment process will be a good option to reduce R_s . Additionally, the high transmittance of graphene remains a key factor when judging the graphene doping strategies. Reducing the R_s of graphene without sacrificing its high transmittance is important for numerous application scenarios, but not for all.

Presently, to incorporate graphene into diverse applications, researchers incessantly explore means to enhance the conductivity of graphene. Aside from the advancements in material preparation strategies and the exploration of key applications, there is also a dearth of standards and mature methodologies to assess the electrical properties of CVD graphene materials. Undoubtedly, the preparation and application demonstrations of highly-conductive CVD graphene materials will not merely bring more thrilling discoveries for fundamental research, but

values in past 16 years. (c) Dependence of R_s on transmittance [20–36, 40, 46, 50, 51, 54–63, 66–69, 86–89].



also drive the progress of the entire graphene-related industry forward.

Data availability statement

No new data were created or analysed in this study.

Acknowledgment

J C Zhang, B Y Mao and H H Liu conceptualize this paper. S L Lv and J C Zhang co-write this paper. W H Lu and J C Zhang designed and drew the schematics. All authors listed have made a substantial, direct, and intellectual contribution to the work, and approved it for publication. This work was supported financially by the National Natural Science Foundation of China (No. 52072042).

ORCID iD

Jincan Zhang https://orcid.org/0000-0002-7131-4491

References

- [1] Zuo X, Chang K, Zhao J, Xie Z, Tang H, Li B and Chang Z 2016 J. Mater. Chem. A 4 51–58
- [2] Yu W, Sisi L, Haiyan Y and Jie L 2020 RSC Adv. 10 15328–45
- [3] Zhou F, Shan J, Cui L, Qi Y, Hu J, Zhang Y and Liu Z 2022 Adv. Funct. Mater. 32 2202026
- [4] Du J, Tong B, Yuan S, Dai N, Liu R, Zhang D, Cheng H and Ren W 2022 Adv. Funct. Mater. 32 2203115
- [5] Liu X et al 2022 Nano Res. 15 3775-80
- [6] Jia K, Zhang J, Zhu Y, Sun L, Lin L and Liu Z 2021 Appl. Phys. Rev. 8 041306
- [7] Singh V, Joung D, Zhai L, Das S, Khondaker S I and Seal S 2011 Prog. Mater. Sci. 56 1178–271
- [8] Tiwari S, Purabgola A and Kandasubramanian B 2020 J. Alloys Compd. 825 153954
- [9] Pezzini S, Mišeikis V, Pace S, Rossella F, Watanabe K, Taniguchi T and Coletti C 2020 2D Mater. 7 041003
- [10] Krasavin S E and Osipov V A 2022 Sci. Rep. 12 14553
- [11] Pavlou C, Pastore Carbone M G, Manikas A C, Trakakis G, Koral C, Papari G, Andreone A and Galiotis C 2021 Nat. Commun. 12 4655
- [12] Fadlalla M I, Kumar P S, Selvam V and Babu S G 2020 J. Mater. Sci. 55 7156–83
- [13] Yin Z, Yang Y, Hu C, Li J, Qin B and Yang X 2024 npg Asia Mater. 16 8
- [14] Xu S et al 2019 Sens. Actuators B 284 125-33

- [15] Xu S et al 2021 Sens. Actuators B 326 128991
- [16] Hu Z, Zhao Y, Zou W, Lu Q, Liao J, Li F, Shang M, Lin L and Liu Z 2022 Adv. Funct. Mater. 32 2203179
- [17] Xu S, Zhang L, Wang B and Ruoff R S 2021 Cell Rep. Phys. Sci. 2 100372
- [18] Ma R et al 2017 Nano Lett. 17 5291-6
- [19] Zhang Y, Tan Y-W, Stormer H L and Kim P 2005 Nature $438\ 201-4$
- [20] Seo Y, Cho H, Jang H, Jang W, Lim J, Jang Y, Gu T, Choi J and Whang D 2018 Adv. Electron. Mater. 4 1700622
- [21] Wei N et al 2019 J. Mater. Chem. A 7 4813-22
- [22] Lin L et al 2019 Nat. Commun. 10 1912
- [23] Jia K et al 2019 J. Am. Chem. Soc. 141 7670-4
- [24] Zhang J et al 2019 Angew. Chem., Int. Ed. 58 14446-51
- [25] Lin L et al 2019 Sci. Adv. 5 eaaw8337
- [26] Jia K et al 2020 Angew. Chem. 132 17367-71
- [27] Jiang B et al 2020 Nano Res. 13 1564-70
- [28] Liu B et al 2021 Nano Res. 14 260-7
- [29] Chen Z et al 2021 Sci. Adv. 7 eabk0115
- [30] Ci H et al 2022 Adv. Mater. 34 2206389
- [31] Shan J et al 2022 Natl Sci. Rev. 9 nwab169 [32] Jiang B et al 2022 Adv. Funct. Mater. 32 2200428
- [33] Liu B et al 2023 Adv. Funct. Mater. 33 2210771
- [34] Liu R et al 2023 Nano Res. 16 6334–42
- [35] Zhang J et al 2023 Nat. Commun. 14 3199
- [36] Tang J et al 2023 Nano Res. 16 10684–9
- [37] Ma T et al 2017 Nat. Commun. 8 14486
- [38] Zhang J, Lin L, Jia K, Sun L, Peng H and Liu Z 2020 *Adv. Mater.* **32** 1903266
- [39] Deng B et al 2017 ACS Nano 11 12337-45
- [40] Zhu Y et al 2023 Adv. Mater. 36 2308802
- [41] Chen H, Zhang J, Liu X and Liu Z 2021 *Acta Phys. Chim. Sin.* 7 10–3866
- [42] Zhang J, Sun L, Jia K, Liu X, Cheng T, Peng H, Lin L and Liu Z 2020 ACS Nano 14 10796–803
- [43] Liu X, Zhang J, Chen H and Liu Z 2021 Acta Phys. Chim. Sin. 38 2012047
- [44] Huang M et al 2020 Nat. Nanotechnol. 15 289-95
- [45] Wang S et al 2023 J. Phys. Chem. C 127 13601-8
- [46] Bianco G V, Sacchetti A, Grande M, D'Orazio A, Milella A and Bruno G 2022 Sci. Rep. 12 8703
- [47] Zhang R, Li M, Li L, Fan Y, Zhang Q, Yu G, Geng D and Hu W 2022 Nano Sel. 3 485–504
- [48] Watson A J, Lu W, Guimarães M H D and Stöhr M 2021 2D Mater. 8 032001
- [49] Song Y, Zou W, Lu Q, Lin L and Liu Z 2021 Small 17 2007600
- [50] Grande M C, Sacchetti A T, Capezzuto P and Bianco G V 2019 Graphene 2019
- [51] Sun L et al 2019 Adv. Mater. 31 1902978
- [52] Kim M-S, Kim M, Son S, Cho S-Y, Lee S, Won D-K, Ryu J, Bae I, Kim H-M and Kim K-B 2020 ACS Appl. Mater. Interfaces 12 30932–40
- [53] Vaziri S, Chen V, Cai L, Jiang Y, Chen M E, Grady R W, Zheng X and Pop E 2020 IEEE Electron Device Lett. 41 1592–5
- [54] Choi M S et al 2021 Nat. Electron. 4 731-9

- [55] Ma L-P et al 2020 Proc. Natl Acad. Sci. 117 25991-8
- [56] Seo Y-M, Jang W, Gu T, Seok H-J, Han S, Choi B L, Kim H-K, Chae H, Kang J and Whang D 2021 ACS Nano 15 11276–84
- [57] Ma L, Dong S, Cheng H and Ren W 2021 Adv. Funct. Mater. 31 2104228
- [58] Zhang Z, Xia L, Liu L, Chen Y, Wang Z, Wang W, Ma D and Liu Z 2021 J. Mater. Chem. C 9 2106–14
- [59] Zhao Y et al 2022 Nat. Commun. 13 4409
- [60] Gao X et al 2022 Nat. Commun. 13 5410
- [61] Ji Im M, Hyeong S-K, Lee J-H, Kim T-W, Lee S-K, Young Jung G and Bae S 2022 *Appl. Surf. Sci.* **605** 154569
- [62] Araki Y et al 2022 ACS Nano 16 14075-85
- [63] Ma L-P, Wu Z, Yan Y, Zhang D, Dong S, Du J, Ma D, Cheng H-M and Ren W 2023 Nano Res. 16 12788–93
- [64] Deokar G, Jin J, Schwingenschlögl U and Costa P M F J 2022 npj 2D Mater. Appl. 6 14
- [65] Yoo M S, Lee H C, Lee S B and Cho K 2021 Adv. Funct. Mater. 31 2006499
- [66] Ma L-P, Dong S, Chen M, Ma W, Sun D, Gao Y, Ma T, Cheng H-M and Ren W 2018 ACS Appl. Mater. Interfaces 10 40756–63
- [67] Kinoshita H, Jeon I, Maruyama M, Kawahara K, Terao Y, Ding D, Matsumoto R, Matsuo Y, Okada S and Ago H 2017 Adv. Mater. 29 1702141
- [68] Xu Y, Yu H, Wang C, Cao J, Chen Y, Ma Z, You Y, Wan J, Fang X and Chen X 2017 Nanoscale Res. Lett. 12 254
- [69] Kim H, Bae S-H, Han T-H, Lim K-G, Ahn J-H and Lee T-W 2014 Nanotechnology 25 014012
- [70] Deng B et al 2015 Nano Lett. 15 4206-13
- [71] Wang K, Shi L, Wang M, Yang H, Liu Z and Peng H 2019 Acta Phys. Chim. Sin. 35 1112–8

- [72] Ullah S, Hasan M, Ta H Q, Zhao L, Shi Q, Fu L, Choi J, Yang R, Liu Z and Rümmeli M H 2019 Adv. Funct. Mater. 29 1904457
- [73] Qi Y, Sun L and Liu Z 2023 Acta Phys. Chim. Sin. 0 2307028
- [74] Qi Y, Sun L and Liu Z 2024 ACS Nano 18 4617-23
- [75] Wang M, Wang L-D, Sheng J, Yang Z-Y, Shi Z-D, Zhu Y-P, Li J and Fei W-D 2019 J. Alloys Compd. 798 403–13
- [76] Mishra N et al 2023 ACS Appl. Eng. Mater. 1 1937–45
- [77] Wang K et al 2022 Nano Res. 15 9727-33
- [78] Cao M et al 2019 Adv. Funct. Mater. 29 1806792
- [79] Zheng H, Zhang R, Xu Q, Kong X, Sun W, Fu Y, Wu M and Liu K 2023 Materials 16 622
- [80] Cui G, Cheng Y, Liu C, Huang K, Li J, Wang P, Duan X, Chen K, Liu K and Liu Z 2020 ACS Nano 14 5938–45
- [81] Liu R et al 2022 Small Methods 6 2200499
- [82] Xie Y et al 2022 Adv. Mater. 34 2202982
- [83] Ramírez C, Shamshirgar A S, Pérez-Coll D, Osendi M I, Miranzo P, Tewari G C, Karppinen M, Hussainova I and Belmonte M 2023 Carbon 202 36–46
- [84] Zeng J, Ji X, Ma Y, Zhang Z, Wang S, Ren Z, Zhi C and Yu J 2018 Adv. Mater. 30 1705380
- [85] Kim S-I et al 2024 Nat. Commun. 15 2172
- [86] Deokar G, Genovese A, Surya S G, Long C, Salama K N and Costa P M F J 2020 Sci. Rep. 10 14703
- [87] Kim K S, Zhao Y, Jang H, Lee S Y, Kim J M, Kim K S, Ahn J-H, Kim P, Choi J-Y and Hong B H 2009 Nature 457 706–10
- [88] Kim D, Lee D, Lee Y and Jeon D Y 2013 *Adv. Funct. Mater.* 23 5049–55
- [89] La Notte L, Villari E, Palma A L, Sacchetti A, Michela Giangregorio M, Bruno G, Di Carlo A, Bianco G V and Reale A 2017 Nanoscale 9 62–69